Evaluation of Photodiode-based Pyranometers and Reference Solar Cells on a Two-Axis Tracking System

Frank Vignola[1], Josh Peterson[1], Rich Kessler[1], Mike Dooraghi[2], Manajit Sengupta[2], and Fotis, Mavromatakis[3]

[1]University of Oregon, Eugene, Oregon, 97403, USA, [2]National Renewable Energy Laboratory, Golden, Colorado, 80401, USA, [3]Technological Educational Institute of Crete, Greece

***Abstract* — The performance of photodiode-based pyranometers and reference solar cells are examined on a two-axis tracker surface. This is the third in a series of papers examining the performance of photodiode-based pyranometers and reference solar cells on fixed and tracking surfaces. Because the instruments are oriented normally to the incident radiation, angle-of-incidence effects are minimized. By removing the angle-of-incidence effects inherent in earlier studies, the change in the sensor's clear sky responsivity can be more clearly identified. It was found that the photodiode-based pyranometers demonstrate a larger change in responsivity than the reference solar cells. Spectral measurements are recommended to verify the cause of this difference.**

***Index Terms* — Pyranometer, reference cell, spectral radiation, two-axis tracking, temperature dependence, systematic bias**

I. Introduction

Photodiode-based pyranometers and reference solar cells are often used to monitor the performance of photovoltaic (PV) systems. These instruments yield different results in the analysis of system performance and it is important to better characterize the strengths and weaknesses of these sensors in monitoring the performance of PV systems. In addition, these instruments are used to estimate the performance of PV systems and it is important to understand any bias introduced by these instruments and to evaluate if adjustments can be made to the data generated by these sensors to remove any biases introduced. This technique has been successfully applied to rotating shadowband radiometers (RSRs) also called rotating shadowband irradiometers (RSI).

In two earlier studies [1], [2] the behavior of photodiode-based pyranometers and reference solar cells was studied on horizontal, fixed-tilt, and one-axis tracking surfaces. The effects of temperature on the sensors was small compared to the effects of changing spectral distribution of the incident radiation and the angle-of-incidence of the irradiance on the sensors. Calibrations of the representative instruments illustrating the magnitude of the various effects are shown in Fig. 1. Models exist for estimating the spectral effects and angle-of-incident effects [3], [4]. The model for the angle-of-incidence effect for the reference cell shown in Fig. 1 did not consider the spectral effects in its development. It is difficult to separate the two affects because they both change as the angle-of-incidence varies.

With a two-axis tracking system, the sensors are normal to the direct irradiance form the sun (DNI), and under sunny skies, the angle-of-incident effects largely disappear. The total (global) irradiance on this two-axis tracking surface (GNI) consists of the DNI plus diffuse irradiance on the normal surface (DfNI) and ground-reflected irradiance on the normal surface (GRNI). DfNI and GRNI do generate angle-of-incident effects, but these effects are expected to be an order of magnitude smaller under clear skies.

II. The Data

The data come from instruments mounted on a two-axis tracker at the Solar Radiation Research Laboratory (SRRL) at the National Renewable Energy Laboratory (NREL). Until December 2017, the (GNI) was measured using a Kipp and Zonen (K&Z) CMP11 pyranometer (responsivity uncertainty of +1.9%/-2.75% (30°-60°). Starting in December 2017, a K&Z CMP22 pyranometer replaced the CMP11. The CMP22 is a secondary standard pyranometer and provides some of the best global and tilted measurements available (uncertainty in responsivity about 1.5% to 60°). Also on the two-axis tracker was a LI-COR LI-200 pyranometer and an IMT reference solar

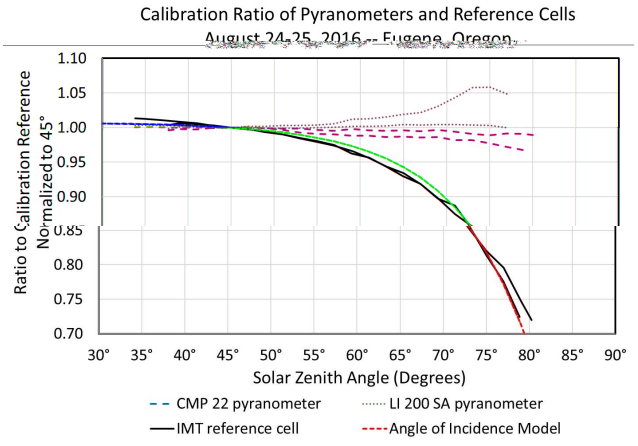

Fig. 1: Calibration of a K&Z CMP-22 (blue dashed line) and LI-200 SA (green dotted line) pyranometer and an IMT reference solar cell (solid black line). The modeled estimate of the angle of incident effect [3] for the reference cell is the red dotted line.

cell. The calibrations of all three instrument were determined by NREL. The reference solar cell was calibrated in the laboratory under a reference lamp and the pyranometers were calibrated under NREL's Broadband Outdoor Radiometer Calibration procedures.

The data are averaged over 1 minute and made available on the NREL midc-srrl-bms website along with other measurements conducted at SRRL. The DNI contribution was measured with a K&Z CHP 1 pyrheliometer operated at SRRL. The accuracy of the DNI data is about 0.7% at the 95% confidence level [5].

The DNI spectral data were obtained from a Prede PGS-100 direct normal spectroradiometer with traceability to National Institute of Standards Technology spectral irradiance lamp standards (through a LICOR LI-1800 spectroradiometer). The instrument has spectral bandwidth of 3.6nm and the detector is maintained at 35°C ± 2°C. The usable spectral range of the instrument is 350-1,050 nm. Measurements are made by a Si-CCD with a 1° field of view. Data are taken at increments of approximately 0.7nm every 5 minutes.

III. Evaluation of the Data

Initial evaluations looked at the ratio of the LI-200A and IMT measurements to the reference GNI measurements under clear-sky conditions. One clear day was selected in summer and another day was selected in winter. It was expected that both would show a dependence on the time of day as the solar zenith angle increased. Models that examine the spectral distribution dependence of the photodiode pyranometers use air mass as a parameter because Rayleigh scattering is dependent on the amount of air the light passes through, preferentially scatters shorter wavelength radiation. Therefore, as the amount of air traversed by light increases, the more the spectral distribution shifts to longer wavelengths [6] (see Fig 2). Because the solar cell used in the LI-200 pyranometer and the IMT reference solar cell are more sensitive to the wavelengths around 900-1000 nm, the responsivity is expected to increase as air mass increases. This is what is seen with the instruments on a two-axis tracker, as shown in Figs. 3 and 4.

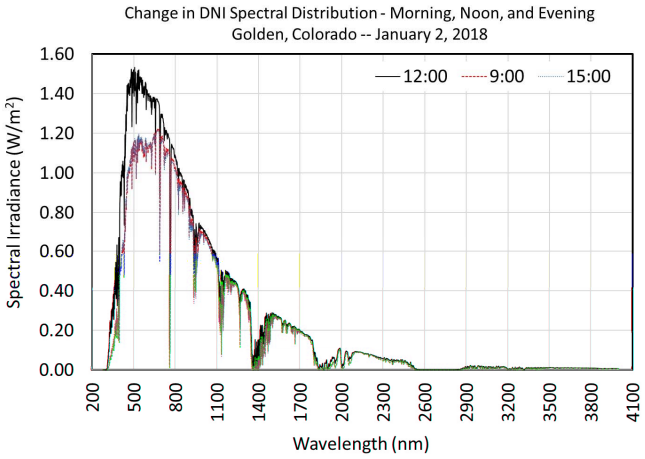

Fig. 2: Change in spectral distribution during the day. Because the sun is lower in the sky in the morning and afternoon compared to noon, the amount of air traversed by the sunlight increases. As the path length through the atmosphere increases, the larger percentage of blue (short wavelength) light is scattered from the DNI. Data at 9:00 and 15:00 are almost identical (dotted red and blue lines. At noon, black line, show a higher percentage of short wavelength irradiance.

As with the photodiode pyranometer on a one-axis tracker [2], the global normal photodiode pyranometer's responsivity increase between 10% and 15% as the air mass increases in the early morning and late afternoon. The increases in responsivity of the reference solar cell is much less, only about 5%. Similar increases in responsivity of reference solar cells were observed for a one-axis tracking system. In the previous study [2], it was postulated that the smaller change in responsivity for a reference solar cell was associated with the spectral effects balancing the effects associated with the change in the angle-of-incidence.

The advantage of the present study is that the instruments are normal to the incident radiation from the sun and only a small amount of the GNI comes from diffuse irradiance and ground reflected irradiance.

The total irradiance on a two-axis tracking surface, GNI, is related to the DNI and the diffuse and ground reflected irradiance by a simple equation.

$$GNI = DNI + DfNI + GRNI \quad (1)$$

where DfNI is the diffuse irradiance on a surface normal to the sun and GRNI is ground-reflected irradiance incident on the two-axis tracking sensor. To get an idea of the percentage of

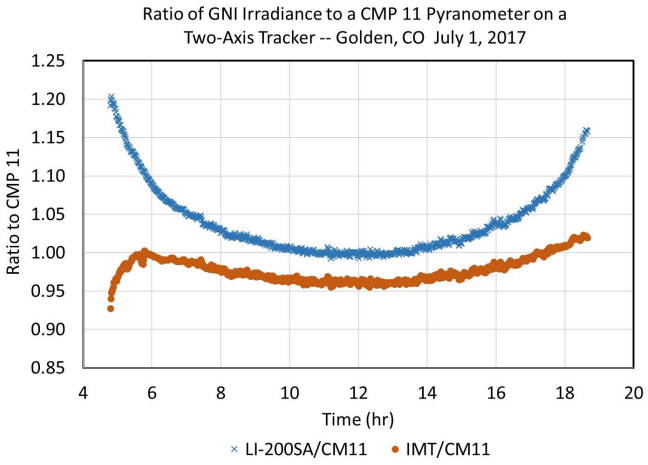

Fig. 3: Plot of the ratio of the LI-200 and IMT reference cell measurements divided by the reference GNI values obtained with a CM11 pyranometer. The Li-200SA ratio data are plotted as blue Xs. The IMT ratio data are plotted as brown Os. Data were obtained on July 1, 2017 under clear-sky conditions. Some data in the morning and evening hours were eliminated because of the obstructions or mountains on the horizon. A few large outliers were eliminated during the day to more clearly show the trends. The 5% difference between the ratios of the two instruments is related to calibrations.

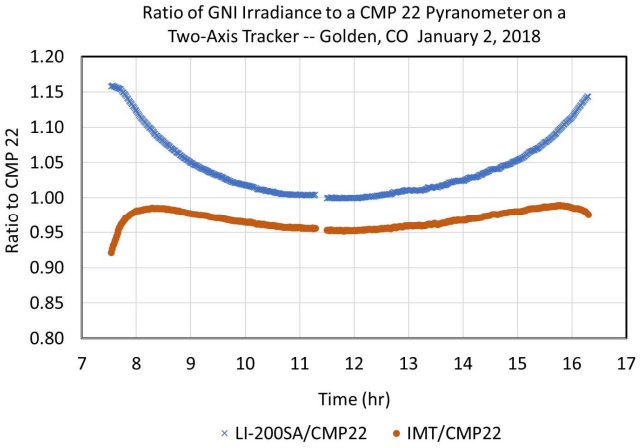

Fig. 4: Plot of the ratio of the LI-200SA and IMT reference cell (brown circles) measurements divided by the reference GNI values obtained with a CM22 pyranometer. The LI-200SA pyranometer data are shown as blue Xs. The IMT reference solar cell data are shown as brown Os. Data were obtained on January 2, 2018, under clear-sky conditions. Data in the very early morning and late evening hours were eliminated because of the obstructions or mountains on the horizon. A few large outliers were eliminated during the day to more clearly show the trends. The 5% different between the LI-2000SA ratios and the IMT reference cell ratios is related to calibrations.

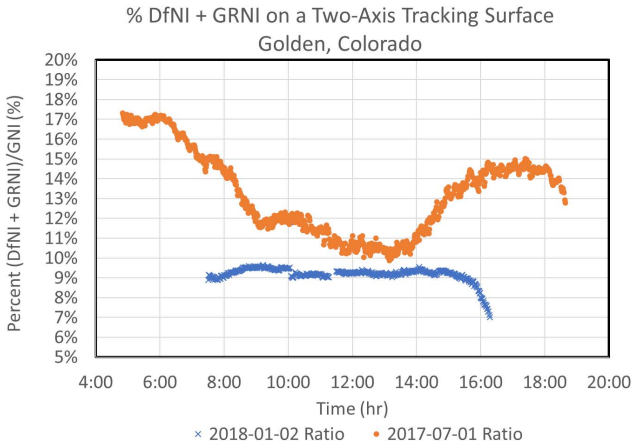

Fig. 5: Plot of the ratio of (GNI-DNI)/GNI on July 1, 2017 (orange circles) and January 2, 2018 (blue x's). Clear sky data. The difference between the GNI and DNI is the DfNI + GRNI. During the day, the percentage of DfNI + GRNI on the two-axis tracking surface varied between 10% and 20%.

irradiance from the DfNI and GRNI compared to the total GNI on a clear day, the DNI was subtracted from the measured GNI and the percentage DfNI + GRNI was plotted against time of day (Fig. 5). For the July 1, 2017 data, the percentage of DfNI + GRNI varied between 10 and 17%. For January 2, 2018, the maximum DfNI + GRNI contribution was about 9.5%. This means that the DNI contributed 80% to 90% of the irradiance incident on the sensors and the angle of incident effects would be relevant only for the DfNI + GRNI irradiance, which only made up 10% to 17% of the total GNI. The portion of the DfNI that came from the sky exhibited only a little angle-of-incidence effect because the diffuse irradiance consists of irradiance from a wide variety of angles. The GRNI becomes more important as the pyranometer's tilt is increased. During the middle of the day, especially in the summer the pyranometer see much less GRNI. The ground-reflected irradiance could have some angle-of-incidence effects, but calibration studies show that angle-of-incident effects become significant only for angles-of-incidence greater than 55° (see Fig. 1).

Therefore, a clear majority of the change in ratios shown in Figs. 3 and 4 are the result of changes in the spectral irradiance, although changes in temperature might play a role. The spectral response of a LI-200SA pyranometer and the IMT reference solar cell is shown in Fig. 6. These responsivities are normalized to one at their peak responsivity. The cell used in the LI 200SA pyranometer has changed over time, and different pyranometers will exhibit different responsivities. The LI-200 SA pyranometer is an older model whereas the IMT reference cell uses much newer technology, hence the slightly higher responsivity.

The spectral responsivity is important because the spectral distribution of incident radiation changes during the day (Fig. 2). An estimate of the effect of changing spectral distribution during the day can be obtained by averaging the responsivity of the instrument times the spectral irradiance and dividing by the sum of the spectral irradiance during the day.

$$\overline{R} = \frac{\sum_{\lambda=200}^{\lambda=4000} I_\lambda \cdot R_\lambda}{\sum_{\lambda=200}^{\lambda=4000} I_\lambda} \qquad (2)$$

where $\overline{R}$ is the average responsivity, and I_λ is the intensity at wavelength λ, and R_λ is the responsivity at wavelength λ. This calculation was carried out using DNI spectral data from Golden, Colorado (shown for January 2, 2018 in Fig. 2) and the

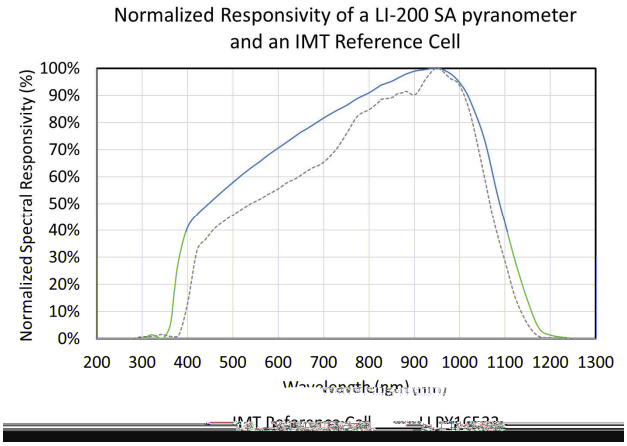

Fig. 6: Relative spectral responsivity of a LI-200SA pyranometer and an IMT reference cell are given in percent normalize to 100% at maximum. The relative spectral response of different pyranometers and reference cells will vary, but the general characteristics are similar. Responsivity data taken at NREL

Table 1: Calculated change in responsivity for a LI-200 SA pyranometer

Date	Time	Average R	Increase in R from Noon	SZA
Jan. 2, 2018	9:00 am	0.4917	1.035	75.96
	Noon	0.4752	----	62.59
	3:00 pm	0.4918	1.035	74.68
July 1, 2017	6:00 am	0.4964	1.052	76.28
	Noon	0.4750	----	16.72
	6:00 pm	0.5028	1.058	74.60

Table 2: Calculated change in responsivity for an IMT reference cell Table 3: Measured ratio of tested instruments

Date	Time	Average R	Increase in R from Noon	SZA
Jan. 2, 2018	9:00 am	0.5781	1.0234	75.96
	Noon	0.5649	----	62.59
	3:00 pm	0.5789	1.0248	74.68
July 1, 2017	6:00 am	0.5856	1.0298	76.28
	Noon	0.5687	----	16.72
	6:00 pm	0.5904	1.0383	74.60

responsivities shown in Fig. 6 at 9:00 a.m., noon, and 3:00 p.m. for January 2, 2018. A similar analysis was done for 6:00 a.m., noon and 6:00 p.m. for July 1, 2017. The results are shown in Table 1 for the LI-200SA pyranometer and Table 2 for the IMT reference cell

The difference between the modeled and measured ratios for the LI-200 SA pyranometer is from 0.3% to 2.5% and for the IMT reference cell from -1.6% to -0.2%. With the uncertainties in the instrument responsivities and irradiance measurements, the spectral dependence of the change is very well established.

Two factors have been neglected. The first is the DfNI and GRNI irradiance that changes during the day, and the second is the effect of temperature. The reference cell does take temperature into account, and the data are adjusted to account for the temperature. At this point, no effects of temperature on the LI-200 SA pyranometer were considered.

If the change in responsivity was totally related to the change in spectral distribution and the assumed spectral responsivity of the instruments were accurate, then one would assume that the change observed in the ratio to the reference instrument shown in Figs. 2 and 3 would be approximately the same as that shown in Tables 1 and 2. The ratios as determined from the data shown in Figs. 2 and 3 are given in Table 3.

The temperature effect is also spectrally sensitive and the effect increases as the energy of the light (longer wavelengths) approaches the energy needed to jump the band-gap for the solar cell (Fig. 7). Often the effects of temperature on the measurements from photodiode pyranometers and reference cells are recorded as average effects over the total measurement. This result fails to consider the change in spectral

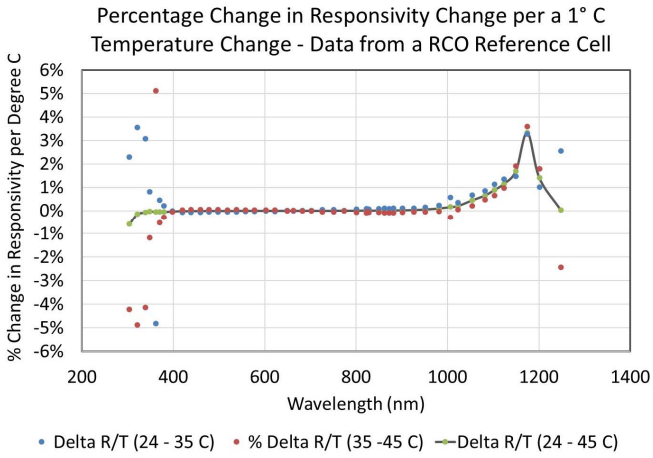

Fig. 7. Typical temperature dependence of a silicon photodiode as a function of wavelength. Data from QE tests taken at NREL at different temperatures.

distribution during the day that would make temperature related effects more prominent in the morning and afternoon as the average spectral distribution shifts to longer wavelengths.

If the spectral dependent temperature effect on the LI-200SA pyranometer were included, the increase responsivity compared to noon would decrease from 1.035 to 1.030 in the morning and increase slightly to 1.036 in the afternoon for the Jan. 2, 2018 comparison and decrease from 1.052 to 1.045 in the morning and increase from 1.058 to 1.059 in the afternoon on July 1, 2017. The effects of temperature in these examples is small in this comparison, but it is likely that there would be a 2% difference in the ratios if one compared the July and January data. For short-circuit current, the output increases with an increase in temperature. This shows up in decrease in responsivity in the morning and the increase in responsivity in the afternoon because the noon time temperature is typically higher than the morning temperature and slightly less than the afternoon temperature.

Models exist that consider the effect of changing spectral distribution during the day. One such model is the King air mass correction formula [King, 1998]. Instead of using the King air mass correction formula, we use the formula:

Table 3: Measured ratio of tested instruments

Date	Time	LI-200SA	IMT	Increase from Noon LI-200SA	Increase from Noon IMT
Jan. 2, 2018	9:00 am	1.050	0.977	1.050	1.025
	Noon	1.000	0.953	----	----
	3:00 pm	1.054	0.981	1.054	1.029
July 1, 2017	6:00 am	1.090	0.997	1.097	1.042
	Noon	0.993	0.956	----	----
	6:00 pm	1.100	1.009	1.108	1.055

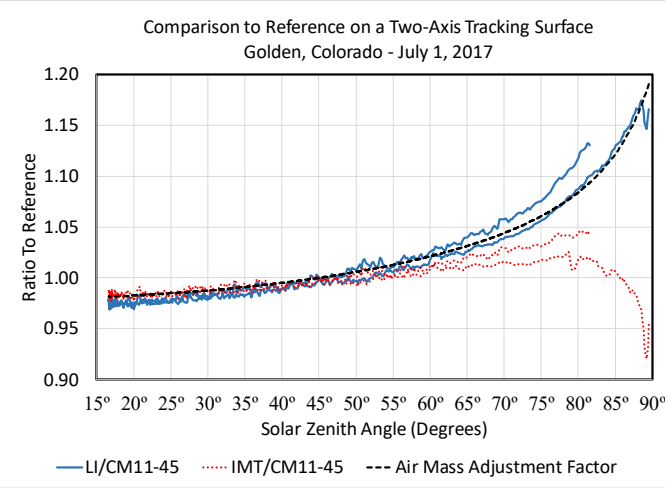

Fig. 8: Ratio of LI-200SA pyranometer (blue line) and IMT reference cell (red dots) to the reference CM 11 pyranometer on a two-axis tracking surface. Modeled spectral adjustment factor is plotted as black dashes. Curves are normalized to 1 at 45º.

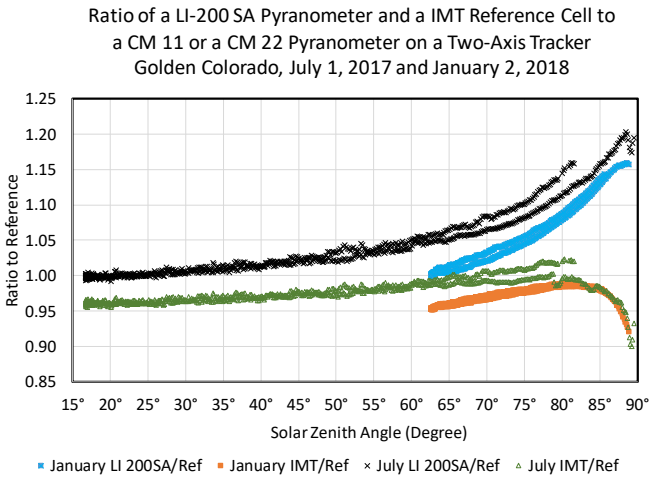

Fig. 9: Comparisons of the ratio of a LI-200SA pyranometer to a CM11 (black Xs) in July or a CM22 in January (blue circles) and an IMT reference cell to a CM11 (green triangles) in July or a CM22 in January (brown Os).

$$F_A = 0.0609 * e^{(\text{Air mass})} + 0.9753 \qquad (3)$$

from [Vignola, 2017]. The two formulas are almost identical from air masses from 1 to 6, but the results from Eq. 3 do not increase as rapidly at higher air masses as the King model results.

The change in the spectral distribution during the day is mainly responsible for the shape of the plots in Fig. 8. The difference between the LI-200SA pyranometer and the IMT reference cell is related to the difference in their spectral distributions. This is similar to the results obtained by King in 1997. At solar zenith angles around 75º, the IMT reference cell ratios start to decrease. At present, the cause for this decrease is under investigation.

The behavior of the instruments should also be compared from summer to winter. This is shown in Fig. 9, which plots similar data but against the solar zenith angle. The data in Fig. 8 are not normalized. Three differences are exhibited here. The ratio of the LI-200 SA to CM11 in summer does not pass through one at 45º. The ratio looks like it could pass through one at 45º with the ratio of the LI-200 SA to CMP22 in January, however, the effect of the temperature difference between July and January would increase the January ratios by about 2%. With the uncertainty in the responsivities determined for the instruments the clear-sky results for the LI-200SA ratios can be considered consistent. More detailed studies are needed to reduce the uncertainties. Similar behavior is found between the IMT reference cell ratios in July and January. The reference cells do take some of the temperature effects into account, but there could be some residual temperature effects that could account for this difference. Alternatively, the difference could be related to the calibration differences between the CMP11 and CMP22 pyranometers.

The reference cells were calibrated in the laboratory under an artificial lamp. The LI-200SA calibration was determined at 45º, as were the K&Z pyranometers. Calibration of the reference cell under standard outdoor pyranometer calibration procedure might reduce this difference. Because PV modules are also calibrated under a standard lamp, this difference might be worth a more thorough examination.

One aspect that is unexplained is the drop of the reference cell ratios at solar zenith angles greater that 75º. One would expect that the ratios would continue to increase similar to the LI-200SA pyranometers. The possibilities for this decrease is possible differential shading of the reference cells or a difference in the ground-reflected irradiance seen by the instruments.

IV. Summary and Future Efforts

This is the third in a series of studies comparing photodiode-based pyranometers and reference cells against thermopile-based pyranometers [1, 2]. This was done for horizontal, fixed tilt, one-axis tracking, and two-axis tracking surfaces. As expected the differences under clear skies are related to the angle-of-incidence effects, changing spectral distributions during the day, and some temperature dependence. As the instrument is moved from horizontal to fixed-tilt to one-axis tracking to two-axis tracking, the effect of the spectral change during the day become more pronounced. This results from the instruments being pointed more directly at the sun in the early morning and later afternoon hours and at these times when the spectral distribution varies most from the noon-time distribution. Having the instruments pointed more directly at the sun as the orientation is changed from horizontal to fixed, to one-axis and then to two-axis tracking surfaces decreases the angle of incident effects. Therefore, tests at different

orientations can help distinguish between angle-of-incidence and spectral effects.

Models exist to account for the angle-of-incidence effects and the effects of changing spectral distribution. These models can be used to remove systematic biases from the measurements on various surfaces, however, the applicability of these models to different locations and the accuracy of these models need further testing. For example, for the two-axis tracking results incorporate the DfNI and GRNI as well as the DNI irradiance. An idea of the magnitude of the influence from effects caused by spectral changes in the DfNI and GRNI can be estimated from Figs. 4 and 5. Because the total contribution of DfNI and GRNI to the GNI compared to the DNI contribution is only about 10% to 15%, it is not expected to significantly affect the results of this study. A 10% change in the DfNI and GRNI would result in only a 1% to 1.5% change in the overall responsivity. That said, it would be interesting to measure the spectral distribution on a one- and two-axis tracking surface to more precisely evaluate the effects of changing spectral distribution. This is also true when studying the spectral effects under cloudy or partially cloudy skies.

The ratio of the GNI from the LI-200SA pyranometer and the IMT reference cell to the reference GNI from the thermopile-based pyranometer could also be improved by using data only from a secondary standard pyranometer such as the CMP22. Data with the improved GNI reference instrument are now being gathered.

V. Conclusions

Both the photodiode-based pyranometer and reference solar cell used in this study exhibit an enhancement in responsivity as the amount of air mass though which light travels increases. The enhancement of the photodiode-based pyranometer is about three times that of the reference solar cell. Do PV modules on two-axis trackers behave like reference solar cells? If so, the photodiode-based pyranometers are likely to overestimate the predicted performance of the modules and underestimate the efficiency of the PV system performance in the morning and evening hours.

PV performance models often have elements that account for the spectral shift over the day. However, the estimates typically depend on accurate irradiance data. Data from instruments that also exhibit a spectral dependence over the day present a possibility of double counting this spectral affect. The temperature adjustment of the model also has a spectral component that should be considered. Therefore, it is important to understand the biases in the input data and how the model handles spectral characteristics of incident radiation and PV model spectral responsivity to accurately assess the model predictions and biases.

One can speculate on the reasons for these differences, but what is really needed is a set of spectral measurements for both irradiance and the responsivity of the photodiode-based pyranometer and the reference solar cell. With that information a more precise evaluation of the effects of spectral distribution can be undertaken. A spectral radiometer is already set up and running at SRRL to evaluate the one-axis tracker and a second system will be installed in Eugene, Oregon to validate the findings at two sites with diverse climates. Additionally, a spectral radiometer will soon be set up in the global normal position at SRRL.

Acknowledgments

This work was supported by the U.S. Department of Energy under Contract No. DE-AC36-08GO28308 with Alliance for Sustainable Energy, LLC, the Manager and Operator of the National Renewable Energy Laboratory. Funding provided by U.S. Department of Energy Office of Energy Efficiency and Renewable Energy Solar Energy Technologies Office. We also thank the other sponsors of the UO Solar Radiation Monitoring Laboratory, the Bonneville Power Administration, and the Energy Trust of Oregon.

References

[1] F. Vignola, C. Chiu, J. Peterson, M. Dooraghi, M. Sengupta, “Comparison and analysis of instruments measuring plane-of-array irradiance for one-axis tracking PV systems”, *IEEE PVSC Conference*, Washington D.C., 2017

[2] F. Vignola, J. Peterson, M. Dooraghi, M. Sengupta, F. Mavromatakis, “Comparison of Pyranometers and Reference Cells on Fixed and One-Axis Tracking” *American Solar Energy Society Conference* Denver, Colorado October 9–12, 2017

[3] B. Marion, “Numerical method for angle-of-incidence correction factors for diffuse radiation incident photovoltaic modules”, Sol. Energy Solar Energy 147 (2017) 344–348

[4] F. Vignola, J. Peterson, S. Wilbert, P. Blanc, N. Geuder, and C. Kern, “New methodology for adjusting rotating shadowband irradiometer measurements” *AIP Conference Proceedings* 1850, 140021 (2017).

[5] A. Habte, M. Sengupta, A. Andreas, S. Wilcox, T. Stoffel, “Intercomparison of 51 radiometers for determining global horizontal irradiance and direct normal irradiance measurements”, Sol. Energy 133, 372-393 2016.

[6] D. King, D. Myers, 1997, Silicon-photodiode pyranometers operational characteristics, historical experiences, and new calibration procedures. In: 26th IEEE Photovoltaic Specialists Conference, September 29 – October 3, 1997, Anaheim, California